International Journal on Future Revolution in Computer Science & Communication Engineering
Volume: 4 Issue: 4

ISSN: 2454-4248
568 – 575

Detection of Hemorrhages and Microaneurysms for Color Fundus Images

Sana Afreen Adbul Farooque, Prof. Pravin Lakhe, Prof. P.D. Bhirange

Department of Electronics and Communication Engg.

SDCE Wardha

Abstract::- Here we address the detection of Hemorrhages and microaneurysms in color fundus images. In pre-Processing we separate red, green, blue color channel from the retinal images. The green channel will pass to the further process. The green color plane was used in the analysis since it shows the best contrast between the vessels and the background retina. Then we extract the GLCM(Gray Level Co-Occurance Matrix) feature. In the GLCMs, several statistics information are derived using the different formulas. These statistics provide information about the texture of an image. Such as Energy, Entropy, Dissimilarity, Contrast, Inverse difference , correlation Homogeneity, Auto correlation, Cluster Shade Cluster Prominence, Maximum probability, Sum of Squares will be calculated for texture image. After feature Extraction, we provide this feature to classifier. Finally it will predict about the retinal whether it is hemorrhages or microaneurysms . After predicting the about the retinal image we will localize the affected place. For segmenting the localized place we will use adaptive thresholding segmentation. .

Keywords: *GLCM, Fundus, Hemorrhages, Microaneurysms*

******

I. Introduction:

Images and pictures

As we mentioned in the preface, human beings are predominantly visual creatures: we rely heavily on our vision to make sense of the world around us. We not only look at things to identify and classify them, but we can scan for differences, and obtain an overall rough feeling for a scene with a quick glance. Humans have evolved very precise visual skills: we can identify a face in an instant; we can differentiate colors; we can process a large amount of visual information very quickly. However, the world is in constant motion: stare at something for long enough and it will change in some way. Even a large solid structure, like a building or a mountain, will change its appearance depending on the time of day (day or night); amount of sunlight (clear or cloudy), or various shadows falling upon it. We are concerned with single images: snapshots, if you like, of a visual scene. Although image processing can deal with changing scenes, we shall not discuss it in any detail in this text. For our purposes, an image is a single picture which represents something. It may be a picture of a person, of people or animals, or of an outdoor scene, or a microphotograph of an electronic component, or the result of medical imaging. Even if the picture is not immediately recognizable, it will not be just a random blur.

II. Aspects of image processing:

It is convenient to subdivide different image processing algorithms into broad subclasses. There are different algorithms for different tasks and problems, and often we would like to distinguish the nature of the task at hand.

- Image enhancement: This refers to processing an image so that the result is more suitable for a particular application.
- Image restoration: This may be considered as reversing the damage done to an image by a known cause.
- Image segmentation: This involves subdividing an image into constituent parts, or isolating certain aspects of an image:

These classes are not disjoint; a given algorithm may be used for both image enhancement or for image restoration. However, we should be able to decide what it is that we are trying to do with our image: simply make it look better (enhancement), or removing damage (restoration).

An image processing task

We will look in some detail at a particular real-world task, and see how the above classes may be used to describe the various stages in performing this task. The job is to obtain, by an automatic process, the postcodes from envelopes. Here is how this may be accomplished:

- Acquiring the image: First we need to produce a digital image from a paper envelope. This can be done using either a CCD camera, or a scanner.
- Preprocessing: This is the step taken before the _major_ image processing task. The problem here is to perform some basic tasks in order to render the resulting image more suitable for the job to follow. In this case it may involve enhancing the contrast, removing noise, or identifying regions likely to contain the postcode.

 ISSN: 2454-4248
568 – 575

- Segmentation: Here is where we actually get the postcode; in other words we extract from the image that part of it which contains just the postcode.
- Representation and description: These terms refer to extracting the particular features which allow us to differentiate between objects. Here we will be looking for curves, holes and corners which allow us to distinguish the different digits which constitute a postcode.
- Recognition and interpretation: This means assigning labels to objects based on their descriptors (from the previous step), and assigning meanings to those labels. So we identify particular digits, and we interpret a string of four digits at the end of the address as the postcode.

III. Literature Survey

The role of hemorrhage and exudates detection in automated grading of diabetic retinopathy

Automated grading has the potential to improve the efficiency of diabetic retinopathy screening services. While disease/no disease grading can be performed using only micro aneurysm detection and image-quality assessment, automated recognition of other types of lesions may be advantageous. This study investigated whether inclusion of automated recognition of exudates and hemorrhages improves the detection of observable/referable diabetic retinopathy. Automated

Automated detection of micro aneurysms in digital red-free photographs: a diabetic retinopathy screening tool

To develop a technique to detect micro aneurysms automatically in 50 degrees digital red-free Fundus photographs and evaluates its performance as a tool for screening diabetic patients for retinopathy. Candidate micro aneurysms are extracted, after the image has been modified to remove variations in background intensity, by algorithms that enhance small round features. Each micro aneurysm candidate is then classified according to its intensity and size by the application of a set of rules derived from a training set of 102 images. An automated technique was developed to detect retinopathy in digital red-free Fundus images that can form part of a diabetic retinopathy screening programme. It is believed that it can perform a useful role in this context identifying images worthy of closer inspection or eliminating 50% or more of the screening population who have no retinopathy.

Automatic detection of red lesions in digital color Fundus photographs

The robust detection of red lesions in digital color Fundus photographs is a critical step in the development of automated screening systems for diabetic retinopathy. In this paper, a novel red lesion detection method is presented based on a hybrid approach, combining prior works by Spencer et al. (1996) and Frame et al. (1998) with two important new contributions. The first contribution is a new red lesion candidate detection system based on pixel classification. Using this technique, vasculature and red lesions are separated from the background of the image. After removal of the connected vasculature the remaining objects are considered possible red lesions. Second, an extensive number of new features are added to those proposed by Spencer-Frame. The detected candidate objects are classified using all features and a k-nearest neighbor classifier. An extensive evaluation was performed on a test set composed of images representative of those normally found in a screening set. When determining whether an image contains red lesions the system achieves a sensitivity of 100% at a specificity of 87%. The method is compared with several different automatic systems and is shown to outperform them all. Performance is close to that of a human expert examining the images for the presence of red lesions.

Automatic detection of micro aneurysms in color Fundus images

This paper addresses the automatic detection of micro aneurysms in color Fundus images, which plays a key role in computer assisted diagnosis of diabetic retinopathy, a serious and frequent eye disease. The algorithm can be divided into four steps. The first step consists in image enhancement, shade correction and image normalization of the green channel. The second step aims at detecting candidates, i.e. all patterns possibly corresponding to MA, which is achieved by diameter closing and an automatic threshold scheme. Then, features are extracted, which are used in the last step to automatically classify candidates into real MA and other objects; the classification relies on kernel density estimation with variable bandwidth. A database of 21 annotated images has been used to train the algorithm. The algorithm was compared to manually obtained grading of 94 images; sensitivity was 88.5% at an average number of 2.13 false positives per image.

Fast detection of the optic disc and fovea in color Fundus photographs.

A fully automated, fast method to detect the fovea and the optic disc in digital color photographs of the retina is presented. The method makes few assumptions about the location of both structures in the image. We define the problem of localizing structures in a retinal image as a regression problem. A KNN repressor is utilized to predict the distance in pixels in the image to the object of interest at any given location in the image based on a set of features measured at that location. The method combines cues measured directly in the image with cues derived from a

 ISSN: 2454-4248
568 – 575

segmentation of the retinal vasculature. A distance prediction is made for a limited number of image locations and the point with the lowest predicted distance to the optic disc is selected as the optic disc center. Based on this location the search area for the fovea is defined. The location with the lowest predicted distance to the fovea within the fovea search area is selected as the fovea location. The method is trained with 500 images for which the optic disc and fovea locations are known. An extensive evaluation was done on 500 images from a diabetic retinopathy screening program and 100 specially selected images containing gross abnormalities. The method found the optic disc in 99.4% and the fovea in 96.8% of regular screening images and for the images with abnormalities these numbers were 93.0% and 89.0% respectively.

IV. Proposed Methodology

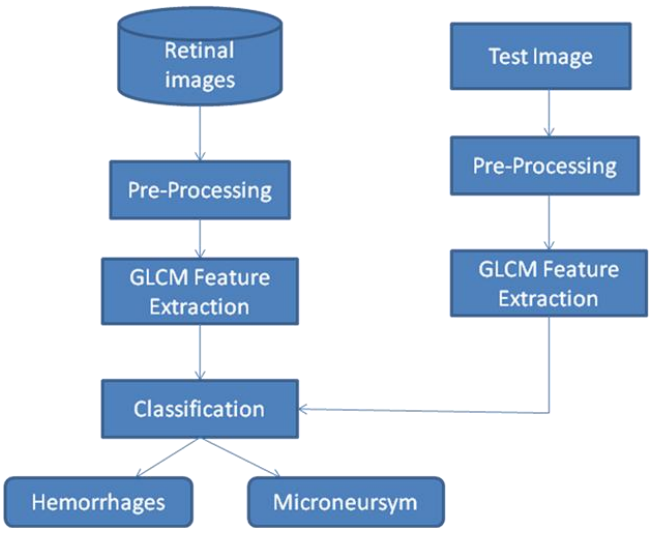

Fig: System Architecture

Pre-Processing:

The green color plane was used in the analysis since it shows the best contrast between the vessels and the background retina. The grey levels were normalized by stretching the image contrast to cover the full pixel dynamic range, excluding the surrounding dark border pixels and any image labels.

Colour Component Separation:

Each image is subjected to colour component separation. Here we separate each image to have three components such as R, G, B. This is an additive colour system based on tri-chromatic theory. Often found in systems that use a CRT to display images. RGB is easy to implement but non–linear with visual perception. It is device dependent and specification of colors is semi–intuitive. RGB is very common, being used in virtually every computer system as well as television, video etc.

V. Feature Extraction:

Gray Level Co-occurrence Matrices

In statistical texture analysis, texture features are computed from the statistical distribution of observed combinations of intensities at specified positions relative to each other in the image. According to the number of intensity points (pixels) in each combination, statistics are classified into first-order, second-order and higher-order statistics.

A GLCM is a matrix where the number of rows and colums is equal to the number of gray levels, G, in the image. The matrix element is the relative frequency with which two pixels, separated by a pixel distance occur within a given neighborhood, one with intensity i and the other with intensity j. One may also say that the matrix element contains the second order statistical probability values for changes between gray levels i and j at a particular displacement distance d and at a particular angle (theta).

A small (5×5) sub-image with 4 gray levels and its corresponding gray level coocrurrence matrix $P(i, j \mid \Delta x = 1, \Delta y = 0)$ is illustrated below.

IMAGE

```
0 1 1 2 3
0 0 2 3 3
0 1 2 2 3
1 2 3 2 2
2 2 3 3 2
```

P(i,j;1,0)

	j=0	1	2	3
i= 0	1/20	2/20	1/20	0
1	0	1/20	3/20	0
2	0	0	3/20	5/20
3	0	0	2/20	2/20

Even visually, quantization into 16 gray levels is often sufficient for discrimination or segmentation of textures.

 ISSN: 2454-4248
568 – 575

Using few levels is equivalent to viewing the image on a coarse scale, whereas more levels give an image with more detail. However, the performance of a given GLCM-based feature, as well as the ranking of the features, may depend on the number of gray levels used.

Because a $G \times G$ matrix (or histogram array) must be accumulated for each sub-image/window and for each separation parameter set (d, θ), it is usually computationally necessary to restrict the (d, θ)-values to be tested to a limited number of values. Figure 1 below illustrates the geometrical relationships of GLCM measurements made for four distances d ($d = max\{|\ \Delta x\ |, |\ \Delta y\ |\}$) and angles of $\theta = 0, \pi/4, \pi/2$ and $3\pi/4$ radians under the assumption of angular symmetry.

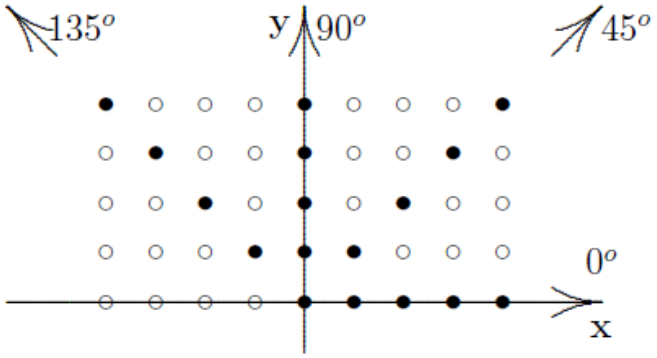

Figure 3. Geometry for measurement of gray level co-occurrence matrix for 4 distances d and 4 angles theta.

In order to obtain a statistically reliable estimate of the joint probability distribution, the matrix must contain a reasonably large average occupancy level. This can be achieved either by restricting the number of gray value quantization levels or by using a relatively large window. The former approach results in a loss of texture description accuracy in the analysis of low amplitude textures, while the latter causes uncertainty and error if the texture changes over the large window. A typical compromise is to use 16 gray levels and a window of about 30 to 50 pixels on each side. Simple relationships exist among certain pairs of the estimated probability distributions P(d, ɵ). Let Pt(d, ɵ) denote the transpose of the matrix P(d, ɵ). Then

$$P(d, 0^0) = P^t(d, 180^0)$$

$$P(d, 45^0) = P^t(d, 225^0)$$

$$P(d, 90^0) = P^t(d, 270^0)$$

$$P(d, 135^0) = P^t(d, 315^0)$$

Thus, the knowledge of P(d, 1800), P(d, 2250), P(d, 2700), and P(d, 3150) adds nothing to the specification of the texture. For a given distance d we usually have four angular gray level co-occurrence matrices.

Texture Features from GLCM

A number of texture features may be extracted from the GLCM

We use the following notation:

G is the number of gray levels used.

μ is the mean value of P.

μx, μy, σ_x and σ_y are the means and standard deviations of Px and Py. Px(i) is the ith entry in the marginal-probability matrix obtained by summing the rows of P(i, j):

 ISSN: 2454-4248
568 – 575

$$P_x(i) = \sum_{j=0}^{G-1} P(i,j)$$

$$P_y(j) = \sum_{i=0}^{G-1} P(i,j)$$

$$\mu_x = \sum_{i=0}^{G-1} i \sum_{j=0}^{G-1} P(i,j) = \sum_{i=0}^{G-1} iP_x(i)$$

$$\mu_y = \sum_{i=0}^{G-1} \sum_{j=0}^{G-1} jP(i,j) = \sum_{j=0}^{G-1} jP_y(j)$$

$$\sigma_x^2 = \sum_{i=0}^{G-1} (i-\mu_x)^2 \sum_{j=0}^{G-1} P(i,j) = \sum_{i=0}^{G-1} (P_x(i) - \mu_x(i))^2$$

$$\sigma_y^2 = \sum_{j=0}^{G-1} (j-\mu_y)^2 \sum_{i=0}^{G-1} P(i,j) = \sum_{j=0}^{G-1} (P_y(j) - \mu_y(j))^2$$

and

$$P_{x+y}(k) = \sum_{i=0}^{G-1} \sum_{j=0}^{G-1} P(i,j) \quad i+j=k \tag{5}$$

for $k = 0, 1, ..., 2(G-1)$.

$$P_{x-y}(k) = \sum_{i=0}^{G-1} \sum_{j=0}^{G-1} P(i,j) \quad |\, i-j \,| = k \tag{6}$$

for $k = 0, 1, ..., G-1$.

The following features are used:

- Homogeneity, Angular Second Moment (ASM) :

$$ASM = \sum_{i=0}^{G-1} \sum_{j=0}^{G-1} \{P(i,j)\}^2 \tag{7}$$

ASM is a measure of homogeneity of an image. A homogeneous scene will contain only a few gray levels, giving a GLCM with only a few but relatively high values of $P(i,j)$. Thus, the sum of squares will be high.

 ISSN: 2454-4248
568 – 575

- Contrast :

$$CONTRAST = \sum_{n=0}^{G-1} n^2 \{ \sum_{i=1}^{G} \sum_{j=1}^{G} P(i,j) \}, \quad |\, i-j \,| = n \tag{8}$$

This measure of contrast or local intensity variation will favour contributions from $P(i,j)$ away from the diagonal, i.e. $i \neq j$.

- Local Homogeneity, Inverse Difference Moment (IDM) :

$$IDM = \sum_{i=0}^{G-1} \sum_{j=0}^{G-1} \frac{1}{1+(i-j)^2} P(i,j) \tag{9}$$

IDM is also influenced by the homogeneity of the image. Because of the weighting factor $(1+(i-j)^2)^{-1}$ IDM will get small contributions from inhomogeneous areas $(i \neq j)$. The result is a low IDM value for inhomogeneous images, and a relatively higher value for homogeneous images.

- Entropy :

$$ENTROPY = -\sum_{i=0}^{G-1} \sum_{j=0}^{G-1} P(i,j) \times log(P(i,j)) \tag{10}$$

Inhomogeneous scenes have low first order entropy, while a homogeneous scene has a high entropy.

- Correlation :

$$CORRELATION = \sum_{i=0}^{G-1} \sum_{j=0}^{G-1} \frac{\{i \times j\} \times P(i,j) - \{\mu_x \times \mu_y\}}{\sigma_x \times \sigma_y} \tag{11}$$

Correlation is a measure of gray level linear dependence between the pixels at the specified positions relative to each other.

- Sum of Squares, Variance :

$$VARIANCE = \sum_{i=0}^{G-1} \sum_{j=0}^{G-1} (i-\mu)^2 P(i,j) \tag{12}$$

This feature puts relatively high weights on the elements that differ from the average value of $P(i,j)$.

- Sum Average :

$$AVER = \sum_{i=0}^{2G-2} i P_{x+y}(i) \tag{13}$$

 ISSN: 2454-4248
568 – 575

- Sum Entropy :

$$SENT = -\sum_{i=0}^{2G-2} P_{x+y}(i) log(P_{x+y}(i)) \quad (14)$$

- Difference Entropy :

$$DENT = -\sum_{i=0}^{G-1} P_{x+y}(i) log(P_{x+y}(i)) \quad (15)$$

- Inertia :

$$INERTIA = \sum_{i=0}^{G-1} \sum_{j=0}^{G-1} \{i-j\}^2 \times P(i,j) \quad (16)$$

- Cluster Shade :

$$SHADE = \sum_{i=0}^{G-1} \sum_{j=0}^{G-1} \{i+j-\mu_x-\mu_y\}^3 \times P(i,j) \quad (17)$$

- Cluster Prominence :

$$PROM = \sum_{i=0}^{G-1} \sum_{j=0}^{G-1} \{i+j-\mu_x-\mu_y\}^4 \times P(i,j) \quad (18)$$

Training the classifier:

A cascade network consists of a cascade architecture, in which hidden neurons are added to the network one at a time and do not change after they have been added. It is called a cascade because the output from all neurons already in the network feed into new neurons. As new neurons are added to the hidden layer, the learning algorithm attempts to maximize the magnitude of the correlation between the new neuron's output and the residual error of the network which we are trying to minimize.

A cascade neural network has three layers: input, hidden and output.

Input Layer: A vector of predictor variable values (x1…xp) is presented to the input layer. The input neurons perform no action on the values other than distributing them to the neurons in the hidden and output layers. In addition to the predictor variables, there is a constant input of 1.0, called the *bias* that is fed to each of the hidden and output neurons; the bias is multiplied by a weight and added to the sum going into the neuron.

Hidden Layer: Arriving at a neuron in the hidden layer, the value from each input neuron is multiplied by a weight, and the resulting weighted values are added together producing a combined value. The weighted sum is fed into a transfer function, which outputs a value. The outputs from the hidden layer are distributed to the output layer.

Output Layer: For regression problems, there is only a single neuron in the output layer. For classification problems, there is a neuron for each category of the target variable. Each output neuron receives values from all of the input neurons (including the bias) and all of the hidden layer neurons. Each value presented to an output neuron is multiplied by a weight, and the resulting weighted values are added together producing a combined value. The weighted sum is fed into a transfer function, which outputs a value. The y values are the outputs of the network. For regression problems, a linear transfer function is used in the output neurons. For classification problems, a sigmoid transfer function is used.

Testing the Selected Input:

Based on the learning of Neural Network, the selected features will be categorizes under one particular category.

 ISSN: 2454-4248
568 – 575

Localization:

First we have to select a gray-level *T* between those two dominant levels, which will serve as a *threshold* to distinguish the two classes (objects and background). Where the value marked as *T* is a natural choice for a threshold. Using this threshold, a new binary image can then be produced, in which objects are painted completely black, and the remaining pixels are white. Denote the original image *f*(*x*, *y*), then the threshold product is achieved by scanning the original image, pixel by pixel, and testing each pixel against the selected threshold: if *f*(*x*, *y*) > *T*, then the pixel is classified as being a background pixel, otherwise the pixel is classified as an object pixel. This can be summarized in the following definition, where *b*(*x*, *y*) denotes the threshold binary image

$$b(x,y) = \begin{cases} 255, \text{if } f(x,y) > T \\ 0, \quad \text{if } f(x,y) \le T \end{cases}$$

In the general case, a threshold is produced for each pixel in the original image; this threshold is then used to test the pixel against, and produce the desired result (in our case, a binary image).

According to this, the general definition of a threshold can be written in the following manner:

$$T = T\,[x, y, p(x, y), f(x, y)]$$

Where *f*(*x*, *y*) is the gray level of point (*x*, *y*) in the original image and p(x, *y*) is some local property of this point (we shall explain this shortly). When *T* depends only on the gray-level at that point, then it degenerates into a simple global threshold (like the ones described in the previous section). Special attention needs to be given to the factor *p*(*x*, *y*). This was described as a property of the point. Actually, this is one of the more important components in the calculation of the threshold for a certain point. In order to take into consideration the influence of noise or illumination, the calculation of this property is usually based on an environment of the point at hand. An example of a property may be the average gray-level in a predefined environment, the center of which is the point at hand.

VI. Conclusion

The automatic detection of the hemorrhages presents various challenges. The hemorrhages are hard to distinguish from background variations because it typically low contrast. Automatic detection of hemorrhage can be confused by other dark areas in the image such as the blood vessels, fovea, and microaneurysms. Hemorrhages have a variable size and often they are so small that can be easily confused with the images noise or microaneurysyms and no standard database that classify hemorrhage by shape. The most false detection is the case when the blood vessels are adjacent or overlapping with hemorrhages. So the effective detection of hemorrhages methodology is needed.

References

[1] S. Wild, G. Roglic, A Green et aI., "Global prevalence of diabetes: estimates for the year 2000 and projections for 2030", Diabetes Care, 27, pp.l047-1053, 2004.

[2] National Eye Institute, National Institutes of Health, "Diabetic Retinopathy: What you should know", Booklet, NIH Publication, No: 06-2171,2003.

[3] Fleming, AD., Goatman, KA, et aI., JA & Scottish Diabetic Retinopathy Clinical Research Network (2010), "The role of haemorrhage and exudate detection in automated grading of diabetic retinopathy", British Journal of Ophthalmology, vol 94, no. 6, pp. 706- 711.

[4] Dupas B, Walter T, Erginay A, et aI., "Evaluation of automated fundus photograph analysis algorithms for detecting microaneurysms, haemorrhages and exudates, and of a computer-assisted diagnostic system for grading diabetic retinopathy", Diabetes Metab, Jun;36(3), pp.213-20., Epub 2010.

[5] G.B. Kande, S.S. Tirumala, P.V. Subbaiah, and M.R. Tagore, "Detection of Red Lesions in Digital Fundus Images", in Proc. ISBI, pp.558-561,2009.

[6] C.Marino, E. Ares , M.G.Penedo, M. Ortega, N. Barreira, F. GomezU1Ia, "Automated Three Stage Red Lesions Detection In Digital Color Fundus Images", WSEAS Transactions on Computers, vol. 7, pp. 207- 215,2008.

[7] M. Esmaeili, H. Rabbani, AM. Dehnavi, and A Dehghani, "A new curvelet transform based method for extraction of red lesions in digital color retinal images", in Proc. ICIP" pp.4093-4096, 2010.

[8] Garcia M, Lopez MI, Alvarez D, Hornero R., "Assessment of four neural network based classifiers to automatically detect red lesions in retinal images", Med Eng Phys. 2010 Dec;32(1O):1085-93. Epub 2010.

[9] Niemeijer M, van Ginneken B, Staal J, Suttorp-SchuItenMSA, Abrmoff MD., "Automatic detection of red lesions in digital color fundus photograph". IEEE Trans Med lmag 24(5):584592, 2005.